J. Fluid Mech. (1980), *vol.* 98, *part* 2, *pp.* 253–271
Printed in Great Britain

Thermally-induced extrudate swell

By H. B. PHUOC AND R. I. TANNER
Department of Mechanical Engineering, University of Sydney,
Sydney 2006, Australia

(Received 22 March 1979 and in revised form 24 September 1979)

In many polymer processing applications, the generation of heat by viscous losses in the flowing molten polymer is highly significant. The heating reduces the viscosity of the melt sharply and the flow patterns are different from the isothermal case. In this paper, a finite element scheme based on the Galerkin method is developed and is used to explore the effects of thermally induced property changes in extrusion.

In the program we solve simultaneously for the flow and temperature fields at each iteration. To check the program for accuracy and correctness, some simple problems were first attempted. A solution for viscous heating in Poiseuille flow was used to check the variable-viscosity part of the program. The crucial convection ('radiation') boundary condition was checked using the solution for cooling of a moving rod. Finally, the swelling of extruded jets with self-heating was investigated. A new phenomenon, thermal extrudate swell, was thereby discovered. We have found extrudate expansions up to 70 % of the die diameter in a Newtonian fluid with thermal properties similar to those of low density polyethylene. It is clear that this phenomenon will affect many experimental interpretations of extrudate swelling.

1. Introduction

When a viscous fluid is extruded through a die into the atmosphere at sufficiently low Reynolds numbers, it is observed that far downstream the extrudate from the die forms a parallel cylinder whose diameter exceeds that of the die. This phenomenon is known as die-swell or extrudate swell. For a creeping Newtonian jet without surface tension or gravity forces, the expansion is about 13 % (Nickell, Tanner & Caswell 1974). The phenomenon is much more marked with non-Newtonian fluids where extrudates can swell up to several times the die diameter. It is usual to attribute this large expansion to fluid visco-elasticity (Tanner 1970) and it is the purpose of this paper to show that this view must be applied cautiously in the most common case of practical interest where molten hot plastic is the extrudate. In such a fluid, Newtonian or otherwise, the variation of viscosity with temperature is an important practical fact (Pearson 1977), and in the present paper we investigate the flow of a Newtonian fluid having a temperature-dependent viscosity in extrusion problems.

This problem does not lend itself to ready analytical solution. These and similar complex flow problems with free surfaces and mixed-boundary conditions appear to require numerical treatment. Here, a finite-element scheme based on the Galerkin discretization procedure is developed to investigate axisymmetric flow problems of

0022-1120/80/4442-8960 $02.00

incompressible, Newtonian, non-isothermal fluids. The full Navier–Stokes and energy equations are used including the nonlinear convective and viscous dissipation terms; the coupling is through the temperature dependent viscosity. The isothermal, Newtonian die-swell problem was treated by Nickell *et al.* (1974) using a similar finite-element scheme. The swelling ratio of about 13 % was in substantial agreement with experiments made at both small finite Reynolds numbers and small ratios of surface tension to viscous forces (Goren & Wronski 1966). The energy equation was included in the works of Tay & de Vahl Davis (1971), Laskaris (1975) and Gartling (1977), amongst others. While the first of these papers used variational methods, weighted residual methods, mainly the Galerkin method, were used in the other works. However, none of these authors dealt with free surface problems; viscous dissipation and convective boundary conditions were also omitted. Thus, this work concentrates on implementing a finite-element scheme incorporating these features, which are necessary for the study of extruded non-isothermal jets.

2. The finite-element scheme

The governing equations for an incompressible, Newtonian, non-isothermal steady fluid flow in component form are:

$$\partial v_j/\partial x_j = 0 \quad \text{continuity;} \tag{1}$$

$$\frac{\partial t_{ij}}{\partial x_j} + \rho\left(f_i - v_j\frac{\partial v_i}{\partial x_j}\right) = 0 \quad \text{momentum;} \tag{2}$$

$$k\frac{\partial^2 T}{\partial x_j\,\partial x_j} - \rho c v_j\frac{\partial T}{\partial x_j} + \mu\Phi = 0 \quad \text{energy.} \tag{3}$$

Here c, k, μ, ρ are respectively the fluid specific heat capacity, thermal conductivity, viscosity, and density and Φ is the viscous dissipation function given by

$$\Phi = \left(\frac{\partial v_i}{\partial x_j} + \frac{\partial v_j}{\partial x_i}\right)\left(\frac{\partial v_i}{\partial x_j}\right). \tag{4}$$

The viscous stress t_{ij} of a Newtonian fluid is

$$t_{ij} = -p\delta_{ij} + \mu\left(\frac{\partial v_i}{\partial x_j} + \frac{\partial v_j}{\partial x_i}\right). \tag{5}$$

The symbols v_i, p, f_i and T have their normal meanings of the velocity component in the x_i direction, pressure, the body force component in the x_i direction, and temperature, respectively. In the present paper, all material parameters (except the viscosity) are held constant.

The boundary surface S is assumed to be

$$S = S_v + S_t = S_T + S_q, \tag{6}$$

where the velocity is given on S_v, stresses on S_t, temperature on S_T and temperature gradient normal to the boundary surface (hence heat flux) on S_q. On S_t, we assume that the boundary force τ_i is given as

$$t_{ij}n_j = \tau_i, \tag{7}$$

where n_j is the outward pointing normal unit vector on the boundary surface. In the present paper, the τ_i are always zero. On S_q, the convection boundary condition is given as

$$\frac{\partial T}{\partial x_j} n_j = -\frac{h}{k}(T - T_\infty) \tag{8}$$
$$= qT + s,$$

where h is the local heat transfer coefficient and T_∞ is the surrounding temperature; q and s are thus simply $-h/k$ and hT_∞/k respectively. Along the boundary surface, τ_i, q and s can vary and are supposed to be known *a priori*.

The Galerkin method is used to discretize the problem. The governing equations (1)–(3) and their boundary conditions (7)–(8) can be written in a general vector form as

$$\mathbf{A}\mathbf{g} = \mathbf{B}, \tag{9}$$

where $\mathbf{A}$ is an operator on the solution vector $\mathbf{g}$ defined by

$$\mathbf{g} = \begin{bmatrix} v_i \\ p \\ T \end{bmatrix}. \tag{10}$$

Aside from the extra variable T and the extra energy equation, the Galerkin treatment is identical to that described for isothermal flows previously (Nickell *et al.* 1974; Tanner, Nickell & Bilger 1975). It will, therefore, be only briefly mentioned here.

In an axisymmetric (or plane) system, we let $\hat{u}_i$, $\hat{w}_i$, $\hat{p}_i$ and $\hat{T}_i$ be respectively the radial (or y) component of velocity, the axial (or x) component of velocity, pressure and temperature at node i; the basic finite element used is a 24 degree-of-freedom quadrilateral composed of four 18 degree-of-freedom triangular sub-elements as shown in figures 1(*a*) and 1(*b*). The computer program first assembles the four triangular sub-elements into a quadrilateral element, then assembles the n quadrilateral elements covering the complete flow field and solves for nodal variables. The solution of the previous iteration is used in the next cycle for an Oseen-linearization of the nonlinear terms in the system.

Pressure p and temperature T are linearly interpolated while the two components u and w are quadratically interpolated; in this way a consistent linear approximation is obtained for the stress field. The interpolation functions are expressed in area co-ordinates ξ_i defined in the usual way and described in previous papers (Nickell *et al.* 1974; Tanner *et al.* 1975).

If we define a vector composed of the functions to be interpolated as

$$\mathbf{v} = \begin{bmatrix} u \\ w \\ p \\ T \end{bmatrix} \tag{11}$$

and arrange the vector $\hat{\mathbf{v}}$ composed of nodal point unknowns as

$$\hat{\mathbf{v}} = [\hat{u}_1, \hat{w}_1, \hat{p}_1, \hat{T}_1, \hat{u}_2, \hat{w}_2, \hat{p}_2, \hat{T}_2, \hat{u}_3, \hat{w}_3, \hat{p}_3, \hat{T}_3, \hat{u}_4, \hat{w}_4, \hat{u}_4, \hat{w}_5, \hat{u}_5, \hat{w}_6]^t \tag{12}$$

then the interpolation polynomial can be written as

$$\mathbf{v} = \boldsymbol{\alpha}(\zeta)\hat{\mathbf{v}}, \tag{13}$$

where $\boldsymbol{\alpha}(\zeta)$ is a $[4 \times 18]$ matrix of interpolation coefficients.

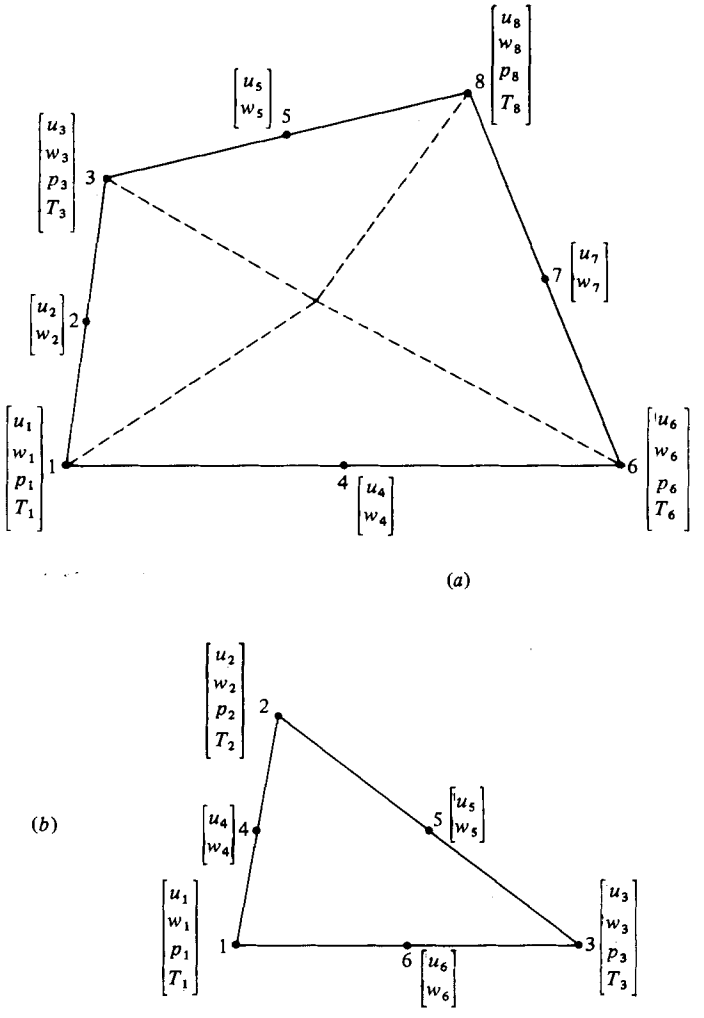

FIGURE 1. The program uses (*a*) a 24 degree-of-freedom quadrilateral element composed of four 18 degree-of-freedom triangular subelements (*b*).

Similarly, we define a vector composed of derivatives of the velocity field and the pressure as

$$\mathbf{e} = \begin{bmatrix} \partial u/\partial r \\ u/r \\ \partial w/\partial z \\ \partial u/\partial z \\ \partial w/\partial r \\ p \end{bmatrix}, \tag{14}$$

which can be written as

$$\mathbf{e} = \boldsymbol{\beta}(\zeta)\hat{\mathbf{v}}, \tag{15}$$

where $\boldsymbol{\beta}(\zeta)$ is a $[6 \times 18]$ matrix of interpolation coefficients.

The constitutive equation for a Newtonian fluid can then be written as

$$\mathbf{t} = \mathbf{D}.\mathbf{e}, \tag{16}$$

where $\mathbf{D}$ is the constitutive matrix

$$\mathbf{D} = \begin{bmatrix} 2\mu & 0 & 0 & 0 & 0 & -1 \\ 0 & 2\mu & 0 & 0 & 0 & -1 \\ 0 & 0 & 2\mu & 0 & 0 & -1 \\ 0 & 0 & 0 & \mu & \mu & 0 \\ 0 & 0 & 0 & \mu & \mu & 0 \\ -1 & -1 & -1 & 0 & 0 & 0 \end{bmatrix}, \tag{17}$$

$\mathbf{t}$ is a column vector $\{t_{rr}\, t_{\theta\theta}\, t_{zz}\, t_{rz}\, t_{rz}\, \Theta\}$, μ is the viscosity and $\Theta = \nabla.\mathbf{v}$.

The nonlinear convective terms are approximated by an Oseen-type approximation as

$$\frac{Du}{Dt} \doteqdot u^* \frac{\partial u}{\partial r} + w^* \frac{\partial u}{\partial z},$$

$$\frac{Dw}{Dt} \doteqdot u^* \frac{\partial w}{\partial r} + w^* \frac{\partial w}{\partial z},$$

where u^* and w^* are the current best estimates of u and w, from the previous iteration. We write the force boundary condition and body force in vector form as

$$\boldsymbol{\gamma} = \begin{bmatrix} \tau_r \\ \tau_z \\ 0 \\ 0 \end{bmatrix}, \qquad \mathbf{f} = \begin{bmatrix} f_r \\ f_z \\ 0 \\ 0 \end{bmatrix}.$$

Then contracting the momentum equation with a virtual field $\boldsymbol{\alpha}\delta\mathbf{v}$ and integrating over space we find (Nickell *et al.* 1974)

$$-\int_V \delta\hat{\mathbf{v}}^t \boldsymbol{\beta}^t \mathbf{D} \boldsymbol{\beta} \hat{\mathbf{v}}\, dV + \int_{S_t} \delta\hat{\mathbf{v}}^t \boldsymbol{\alpha}^t \boldsymbol{\gamma}\, dS + \int_V \delta\hat{\mathbf{v}}^t \boldsymbol{\alpha}^t \mathbf{f}\, dV - \int_V \delta\hat{\mathbf{v}}^t \boldsymbol{\alpha}^t \boldsymbol{\Phi} \boldsymbol{\beta} \hat{\mathbf{v}}\, dV = 0, \tag{18}$$

where

$$\boldsymbol{\Phi} = \begin{bmatrix} \rho u^* & 0 & 0 & \rho w^* & 0 & 0 \\ 0 & 0 & \rho w^* & 0 & \rho u^* & 0 \\ 0 & 0 & 0 & 0 & 0 & 0 \\ 0 & 0 & 0 & 0 & 0 & 0 \end{bmatrix}.$$

We treat the energy equation (3) similarly; we multiply by an interpolation function and use the divergence theorem, taking account of the boundary condition (8) on part of the boundary of the fluid. We can write the components of the temperature gradient and the temperature in the form

$$\begin{bmatrix} \dfrac{\partial T}{\partial r} \\ \dfrac{\partial T}{\partial z} \end{bmatrix} = \mathbf{Z}.\hat{\mathbf{v}}, \tag{19}$$

$$T = \mathbf{Y}.\hat{\mathbf{v}}, \tag{20}$$

where $\mathbf{Z}$ and $\mathbf{Y}$ are simple matrices, and replace DT/Dt and the dissipation function by an Oseen-type approximation as

$$\frac{DT}{Dt} \doteq u^* \frac{\partial T}{\partial r} + w^* \frac{\partial T}{\partial z}$$
$$\doteq u^* \mathbf{C}_r \hat{\mathbf{v}} + w^* \mathbf{C}_z \hat{\mathbf{v}}, \tag{21}$$

where $\mathbf{C}_r$ and $\mathbf{C}_z$ are also simple matrices.

Then contracting the energy equation with a virtual field and integrating over V we obtain

$$-\int_V \frac{k}{\rho c} \delta\hat{\mathbf{v}}^t \mathbf{Z}^t \mathbf{Z} \hat{\mathbf{v}}\, dV + \int_{S_q} \frac{kq}{\rho c} \delta\hat{\mathbf{v}}^t \mathbf{Y}^t \mathbf{Y} \hat{\mathbf{v}}\, dS + \int_V \frac{ks}{\rho c} \delta\hat{\mathbf{v}}^t \mathbf{Y}^t\, dS$$
$$+ \int_V \frac{\mu}{\rho c} \delta\hat{\mathbf{v}}^t \mathbf{Y}^t \mathbf{e}^{*t} \mathbf{E} \boldsymbol{\beta} \hat{v} dV - \int_V \delta\hat{\mathbf{v}}^t \mathbf{Y}^t (u^* \mathbf{C}_r + w^* \mathbf{C}_z)\, \hat{\mathbf{v}}\, dV = 0, \tag{22}$$

where $\mathbf{e}^*$ is given by (15) (evaluated at the previous interation) and $\mathbf{E}$ is given by

$$\mathbf{E} = \begin{bmatrix} 2 & 0 & 0 & 0 & 0 & 0 \\ 0 & 2 & 0 & 0 & 0 & 0 \\ 0 & 0 & 2 & 0 & 0 & 0 \\ 0 & 0 & 0 & 1 & 1 & 0 \\ 0 & 0 & 0 & 1 & 1 & 0 \\ 0 & 0 & 0 & 0 & 0 & 0 \end{bmatrix}. \tag{23}$$

Now, by summing (18) and (22) and eliminating the vector of arbitrary constants $\delta\hat{\mathbf{v}}^t$, the stiffness-force equation for a triangular sub-element can be written as

$$\mathbf{K} . \hat{\mathbf{v}} = \mathbf{F}, \tag{24}$$

where

$$\mathbf{K} = \int_V \boldsymbol{\beta}^t \mathbf{D} \boldsymbol{\beta}\, dV + \int_V \boldsymbol{\alpha}^t \boldsymbol{\Phi} \boldsymbol{\beta}\, dV - \int_V \frac{k}{\rho c} \mathbf{Z}^t \mathbf{Z}\, dV + \int_V \frac{kq}{\rho c} \mathbf{Y}^t \mathbf{Y}\, dS$$
$$+ \int_V \frac{\mu}{\rho c} \mathbf{Y}^t \mathbf{e}^{*t} \mathbf{E} \boldsymbol{\beta}\, dV - \int_V \mathbf{Y}^t (u^* \mathbf{C}_r + w^* \mathbf{C}_z)\, dV \tag{25}$$

and

$$\mathbf{F} = \int_{S_t} \boldsymbol{\alpha}^t \boldsymbol{\gamma}\, dS + \int_V \boldsymbol{\alpha}^t \mathbf{f}\, dV - \int_{S_q} \frac{ks}{\rho c} \mathbf{Y}^t\, dS. \tag{26}$$

In the evaluation of the volume integrals in (25) and (26) a 7-point Gaussian integration scheme was used (Nickell *et al.* 1974); the surface integrals were evaluated analytically.

The matrix $\mathbf{K}$ is not symmetric and at each iteration the unsymmetric system was solved; it has not been found possible to secure convergence with some of the schemes designed to use a symmetric matrix mentioned by Nickell *et al.* (1974). The updating of the free surface is also performed by the method described by Tanner *et al.* (1975).

3. Solution to some simple problems

The program was checked for correct operation and accuracy by solving problems with known exact solutions. The first check was Poiseuille flow with heat transfer, and a viscosity of the form

$$\mu = \mu_0 \exp -\alpha T, \tag{27}$$

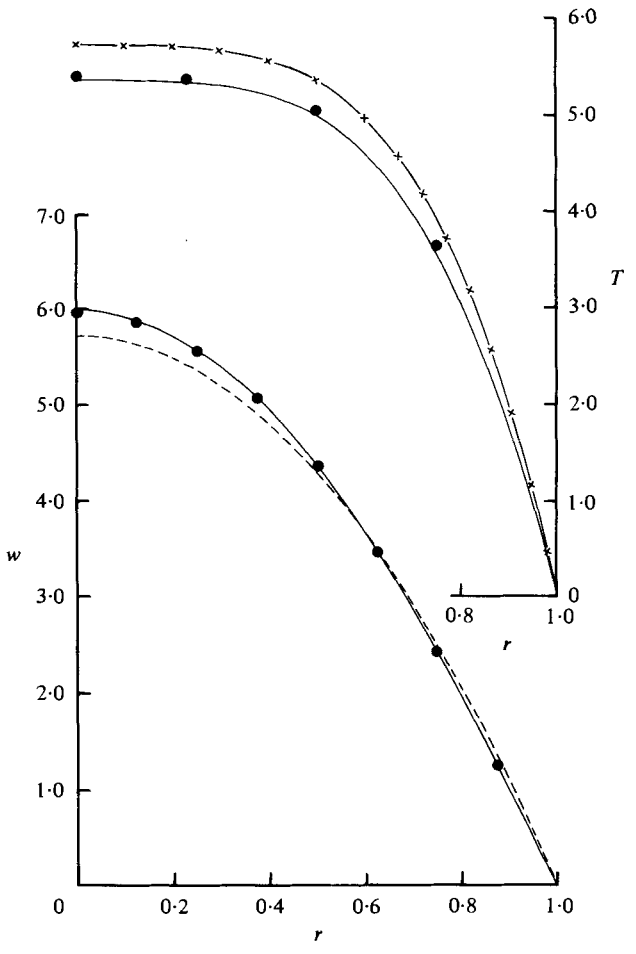

FIGURE 2. Temperature [equation (29)] and velocity [equation (28)] profiles for Poiseuille problem with self-heating. ——, exact solutions; ●, finite-element solution with 4 elements in radial and axial directions; – – –, velocity profile for constant viscosity and same discharge; × — ×, temperature profile for $\alpha = 0$ (constant viscosity).

where μ_0 and α are constants. The analytical solution of this problem given by Kearsley (1962) is

$$w = \frac{4R^2P_z}{\mu_0}\left\{\frac{1}{K+\gamma} - \frac{r^{*2}}{Kr^{*4}+\gamma} + \frac{1}{(K\gamma)^{\frac{1}{2}}}\tan^{-1}\frac{(K\gamma)^{\frac{1}{2}}(1-r^{*2})}{\gamma+Kr^{*2}}\right\} \tag{28}$$

and

$$T = \alpha^{-1}\ln\left[32\gamma/(Kr^{*4}+\gamma)^2\right], \tag{29}$$

where P_z is the pressure gradient, R the tube radius, k the thermal conductivity, $K = \alpha R^4P_z^2/4\mu_0 k$ the non-dimensional measure of viscous heating, $r^* = r/R$, a dimensionless radial co-ordinate, and $\gamma \equiv 16 - K + 4(16-2K)^{\frac{1}{2}}$. If $K = 0$, we revert to the parabolic Poiseuille profile for w and the quartic profile for T, which are plotted in figure 2.

The numerical iteration was started from the Poiseuille solution ($\alpha = 0$) and converged in 4 iterations. Figure 2 shows a satisfactory comparison between exact

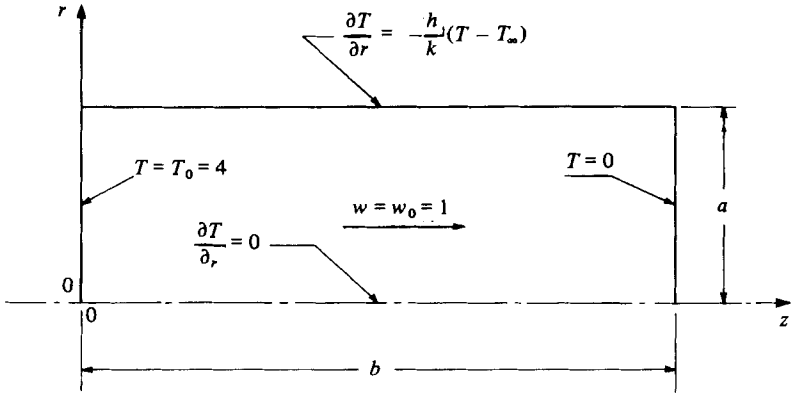

FIGURE 3. Test problem: the cooling of a moving solid rod with both fixed temperature (ends) and convective boundary conditions (curved surface).

solutions and finite element solutions for $K = 3{\cdot}5$. This comparison of the axial velocity profiles and temperature profiles, when using 4 elements in both the radial and axial directions showed errors of less than 0·8 % and 1·2 % in the axial velocity and temperature fields respectively.

In the above problem, the temperature of the tube wall is maintained constant, and the heat transfer boundary condition (8) does not operate. To test this part of the program, we considered the problem of a moving cylindrical rod cooled by convection. The problem is sketched in figure 3 and the temperature field admits an exact solution in terms of J_0, the zero-order Bessel function.

Suppose the cylindrical rod of radius a and length b moves axially at a constant velocity $w = w_0$. At $z = 0, T = T_0$ and at $z = b, T$ is zero. The rod is cooled by convection on $r = a$. Thus, the boundary conditions are:

(*a*) $T = T_0$ on $z = 0$;

(*b*) $T = 0$ on $z = b$;

(*c*) on the surface $r = a$,

$$\frac{\partial T}{\partial r} = \frac{-h}{k}(T - T_\infty), \tag{30}$$

here we take $T_\infty = 0$ (thus h is the surface heat transfer coefficient and k is the thermal conductivity of the rod);

(*d*) along the axis of symmetry $r = 0$ we have $\partial T/\partial r = 0$;

(*e*) $w = w_0, u = 0$ on all rod boundaries, this defines the rigid body motion.

It may easily be shown (Phuoc 1978) that the temperature T is given by

$$\frac{T}{T_0} = \sum_{n=1}^{\infty} \frac{2}{a\alpha_n}\left(\frac{h}{k\alpha_n}\right) \frac{J_0(r\alpha_n)\exp z[\beta + (\beta^2 + \alpha_n^2)^{\frac{1}{2}}]}{(1 + (h^2/k^2\alpha_n^2))\, J_0(a\alpha_n)} \left\{\frac{1 - e^{2(b-z)(\beta^2+\alpha_n^2)^{\frac{1}{2}}}}{1 - e^{2b}(\beta^2+\alpha_n^2)^{\frac{1}{2}}}\right\}, \tag{31}$$

where α_n are the roots of

$$J_1(\alpha a_n) = \left(\frac{h}{k\alpha_n}\right) J_0(a\alpha_n) \tag{32}$$

and $\beta \equiv \rho c w_0/2k$. Here ρ is the material density and c is the specific heat. As a test problem we used ha/k (a Nusselt number) = 2, $\beta = 0{\cdot}5$ inverse length units, $b = 3$

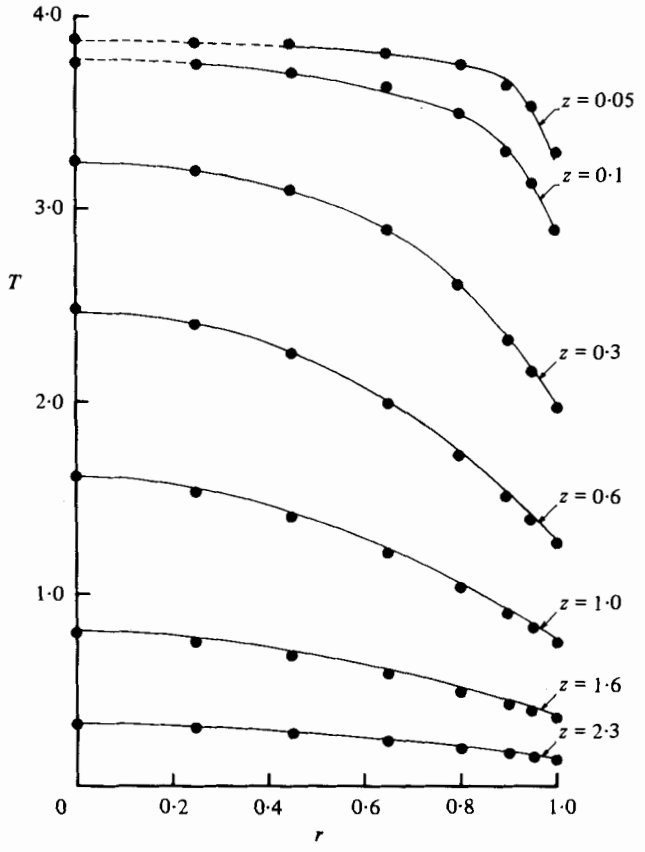

FIGURE 4. Temperature profiles in a moving rod cooled by convection. ——, exact solution, first six terms of (31); ●, finite-element solution (7 × 8 elements); – – –, estimated solution – first six terms of (31) not sufficiently accurate in this region.

length units, $a = 1$ length unit, and $T_0 = 4$ temperature units. Six terms of the series were used to evaluate (31) and in some regions this is not sufficient (dotted lines in figure 4). The comparison in figure 4 was considered to be a satisfactory approximation to the exact solution.

Several other problems with variable viscosity were solved (Phuoc 1978) including the cooling of a two-dimensional slab and the Graetz problem (flow in a circular tube with a step change in wall temperature at a given plane). In all cases the numerical and analytical solutions were in satisfactory agreement.

4. Non-isothermal extrusion

We now consider the extrusion of an incompressible Newtonian fluid (see figures 5–8) where the viscosity μ is assumed to vary with temperature according to

$$\mu = \bar{\mu} \exp\{-\alpha(T - T_w)\}. \tag{33}$$

A sketch of the problem is shown in figure 5. The basic scaling parameters are: tube radius R, average fluid velocity in pipe $\bar{w}$, pipe wall temperature T_w, ambient temperature T_∞, fluid viscosity at T_w, $\bar{\mu}$.

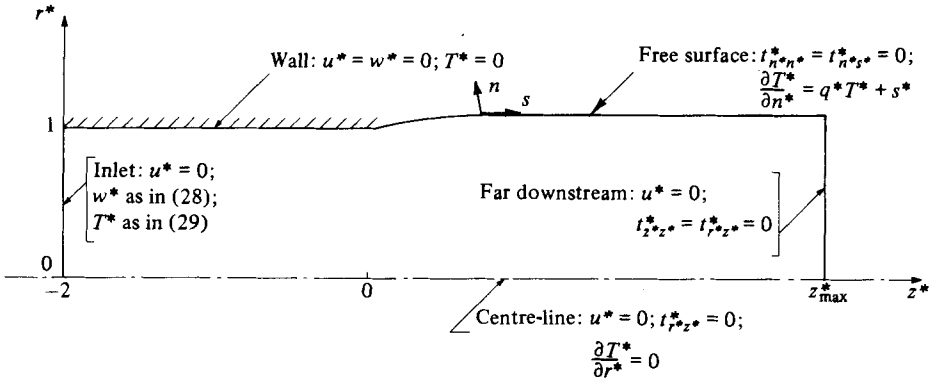

FIGURE 5. Boundary conditions for extrudate swell problem.

We may then define the non-dimensional parameters:

$$u^* = u/\bar{w}; \quad w^* = w/\bar{w}; \quad r^* = r/R; \quad z^* = Z/R;$$

$$p^* = \frac{pR}{\bar{\mu}\bar{w}}; \quad \rho^* = \frac{\rho \bar{w} R}{\bar{\mu}}; \quad T^* = \frac{T - T_w}{T_w - T_\infty};$$

$$c^* = \frac{c(T_w - T_\infty)}{\bar{w}^2}; \quad k^* = \frac{k(T_w - T_\infty)}{\bar{\mu}\,\bar{w}^2}; \quad \alpha^* = \alpha(T_w - T_\infty); \quad \mu^* = \frac{\mu}{\bar{\mu}}.$$

Then the non-dimensional continuity, momentum and energy equations in an axisymmetric co-ordinate system are written in terms of these dimensionless variables. Note that ρ^* is a Reynolds number; α^*, k^* and c^* are also dimensionless parameters characterizing the problem. An additional parameter (gravity, air drag and surface tension are ignored here) which also influences the solution is the convective heat transfer coefficient for the jet, through the Nusselt number hR/k. Here we shall not attempt to compute all the possibilities among this field of parameters. Instead we shall consider a Newtonian fluid with properties corresponding to those of low-density polyethylene, and consider the extrusion through a long die of radius 1 mm. Thus we take (Phuoc 1978)

$$R = 1\,\text{mm}, \quad \rho = 0{\cdot}92\,\text{mg/mm}^3, \quad k = 0{\cdot}335\,\text{W/m °K}, \quad c = 2{\cdot}3\,\text{kJ/kg °K}.$$

The wall and ambient temperatures are chosen to be $T_w = 150\,°\text{C}$, $T_\infty = 25\,°\text{C}$. Around a temperature of 150 °C, the viscosity can be approximated by

$$\mu = 9{\cdot}306 \times 10^9 e^{-0{\cdot}0342(T)}\,\text{mg mm}^{-1}\,\text{s}^{-1}.$$

The viscosity at $T_w = 150\,°\text{C}$ is $\bar{\mu} = 5{\cdot}5 \times 10^7\,\text{mg mm}^{-1}\,\text{s}^{-1}$ which gives the non-dimensional viscosity as

$$\mu^* = e^{-4{\cdot}276T^*}. \tag{34}$$

With $\bar{w}$ varying between 1 mm s^{-1} and 30 mm s^{-1} the Peclet number varies between 6·3 and 190 and the Reynolds number is less than 10^{-5}.

The non-dimensional thermal boundary condition on the free surface is given by

$$\partial T^*/\partial n^* = q^* T^* + s^*$$

with $s^* = q^* = -(h/k)R$; n is the outward-pointing normal vector to the free surface.

Acierno *et al.* (1971) measured $(h/k)\,R$ for polyethylene and found that very close

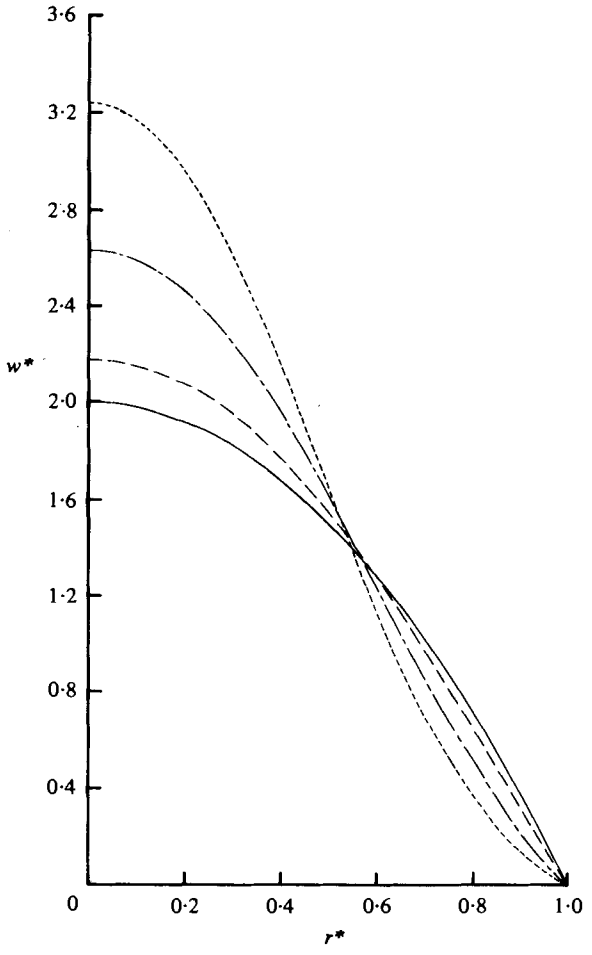

FIGURE 6. Dimensionless input velocity profiles for various flow rates. ——, $\bar{w} = 1\,\mathrm{mm\,s^{-1}}$; – – –, $\bar{w} = 10\,\mathrm{mm\,s^{-1}}$; —·—, $\bar{w} = 20\,\mathrm{mm\,s^{-1}}$; - - - - -, $\bar{w} = 30\,\mathrm{mm\,s^{-1}}$.

to the spinneret and in still air, $(h/k)\,R$ is constant and equal to 0·72. We adopt this value as an approximation to our heat transfer coefficient in this example. Thus

$$s^* = q^* = -0{\cdot}72.$$

The boundary conditions for the extrusion problem are then as follows (figure 5).

(*a*) At inlet, i.e. along $z^* = -2$, the fully-developed velocity and temperature profiles of a viscously heated fluid as given by Kearsley (1962) are prescribed; thus we use (28) and (29) as input profiles. These are shown in figures 6 and 7 in dimensionless form.

(*b*) Along the pipe wall, i.e. $r^* = 1$ $(0 < z^*)$, we prescribe the no-slip boundary condition $u^* = w^* = 0$ and the isothermal wall condition $T^* = 0$ (corresponding to $T = T_w = 150\,^\circ\mathrm{C}$).

The non-dimensional flow rate is given by

$$Q^* = \frac{4\pi R^* p_z^*}{\mu_0^*(K+\gamma)} = \pi. \tag{35}$$

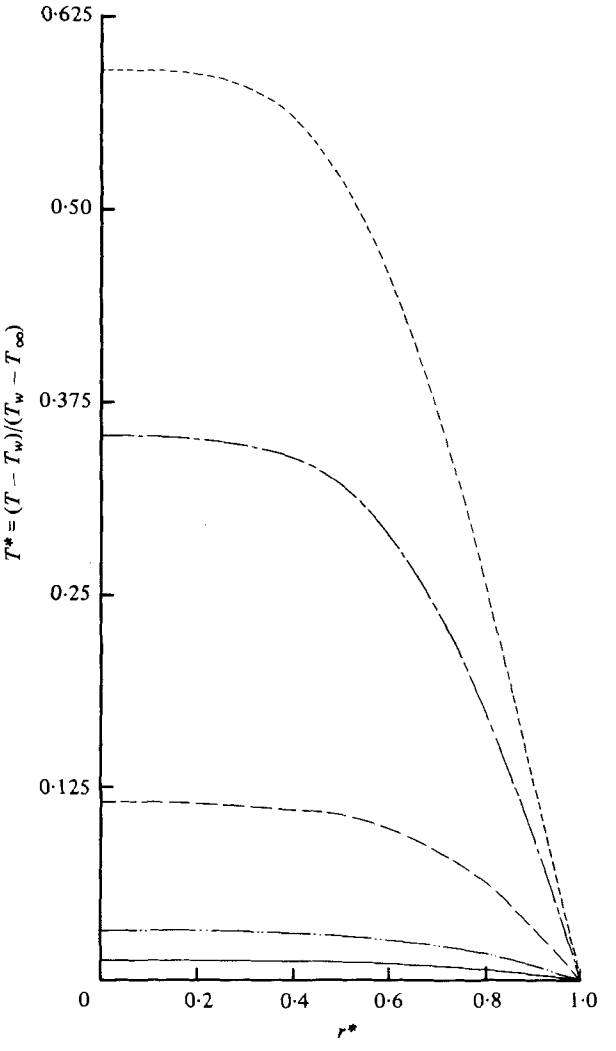

FIGURE 7. Dimensionless input temperatures profiles for various flow rates. ——, $\bar{w} = 1\,\mathrm{mm\,s^{-1}}$; –·–·–, $\bar{w} = 5\,\mathrm{mm\,s^{-1}}$; – – –, $\bar{w} = 20\,\mathrm{mm\,s^{-1}}$; – – –, $\bar{w} = 20\,\mathrm{mm\,s^{-1}}$; · · · · ·, $\bar{w} = 30\,\mathrm{mm\,s^{-1}}$.

(*c*) Along the free surface we have no stresses, $t^*_{n^*n^*} = t^*_{n^*s^*} = 0$, and the convection boundary condition, $\partial T^*/\partial n^* = -0{\cdot}72T^* - 0{\cdot}72$.

(*d*) Far downstream (where z^* is sufficiently large so that there is no further change in the extrudate diameter), we impose zero radial velocity and axial stress, $u^* = 0$, $t^*_{z^*z^*} = 0$. No thermal boundary condition is imposed on this end, thus the solution attempts to make $\partial T/\partial z$ zero here. This is discussed further below.

(*e*) Along the centre-line, i.e. $r^* = 0$, we impose no radial velocity and no shear stress, $u^* = 0$, $t^*_{r^*z^*} = 0$, and an axis of symmetry boundary condition for temperature, $\partial T^*/\partial r = 0$.

With this set of boundary conditions and the element pattern shown in figure 8, a series of five computer runs was made with $\bar{w} = 1\,\mathrm{mm\,s^{-1}}$, $5\,\mathrm{mm\,s^{-1}}$, $10\,\mathrm{mm\,s^{-1}}$,

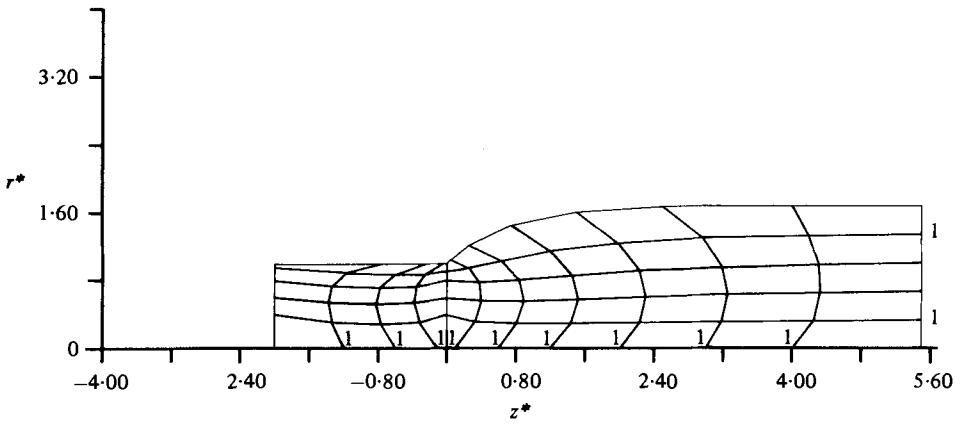

FIGURE 8. Element pattern used for solution of extrusion problem.

20 mm s^{-1} and 30 mm s^{-1}. About 20 iterations were needed for convergence at the largest speed (Péclet number of about 190).

An expansion ratio can be defined by

$$\epsilon = r^*_{\max}/R - 1$$

where $r^*_{\max}$ is the filament radius far downstream. Figure 9 shows that ϵ increases from 13·4 % to 69·4 % as $\overline{w}$ increases from 1 mm s^{-1} to 30 mm s^{-1}. It can also be seen that as $\overline{w} \to 0$, the expansion ratio ϵ tends to about 13 % in agreement with established data (Nickell *et al.* 1974; Goren & Wronski 1966). The upper limit of $\overline{w} = 30$ mm s^{-1} was set by considering the maximum temperature that polyethylene may experience without oxidation; this velocity corresponds to a maximum temperature of about 224 °C, which is close to the 230 °C oxidation temperature of polyethylene. However, there appears to be no natural limit to the thermal swelling at this point and it simply is the point at which computing was stopped. The Péclet number varies linearly with $\overline{w}$ so that

$$Pe = \frac{\rho c \overline{w} R}{k} = 6{\cdot}324\overline{w} \quad (\overline{w} \text{ in mm s}^{-1}).$$

The Péclet number assumes values up to about 190 for $\overline{w} = 30$ mm s^{-1}; the Reynolds number Re is $2\rho\overline{w}R_0/\mu \simeq 0{\cdot}3 \times 10^{-7}\overline{w}$, and is always negligible here.

Figures 10–12 show the contours of stream function, pressure and temperature for the $\overline{w} = 30$ mm s^{-1} case. The velocity and stress contours are similar to those previously published (Nickell *et al.* 1974) and are not repeated here.

Figure 13 shows the temperature contours for the slowest jet ($\overline{w} = 1$ mm s^{-1},or Péclet number of 6·3). The arbitrary imposition of the free zero-gradient boundary condition on the downstream face ($z^* = 3$) needs some discussion. Because the cooling of the filament is so slow, it is not practical to solve the problem with a jet long enough to reach ambient temperature, at least at higher extrusion rates. Actually, the problem for large z becomes identical to the cooling of a solid rod, as all mechanical rearrangements seem to be complete within about 1·2 jet radii from the exit. We can use the

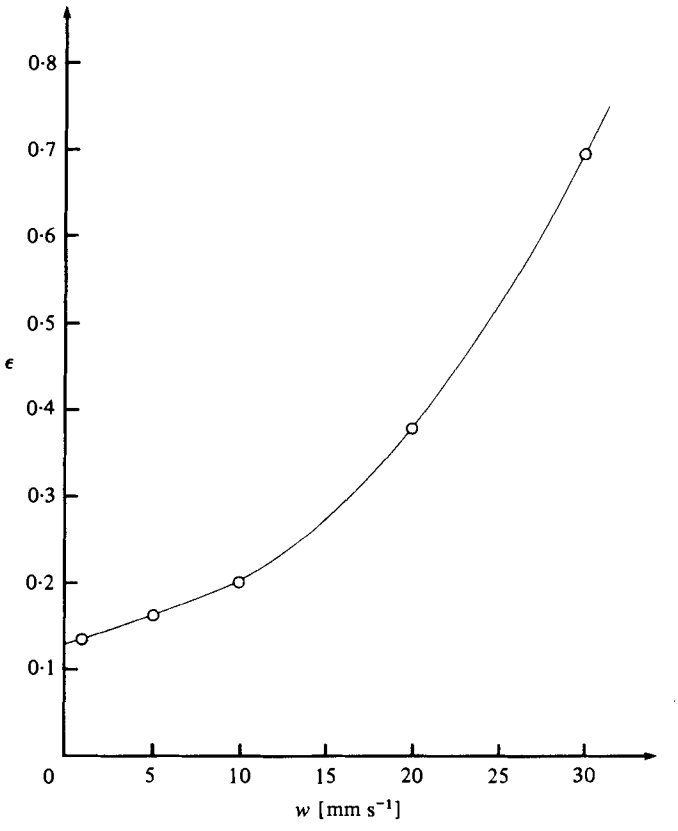

FIGURE 9. Expansion ratio ϵ as a function of mean velocity $\overline{w}$.

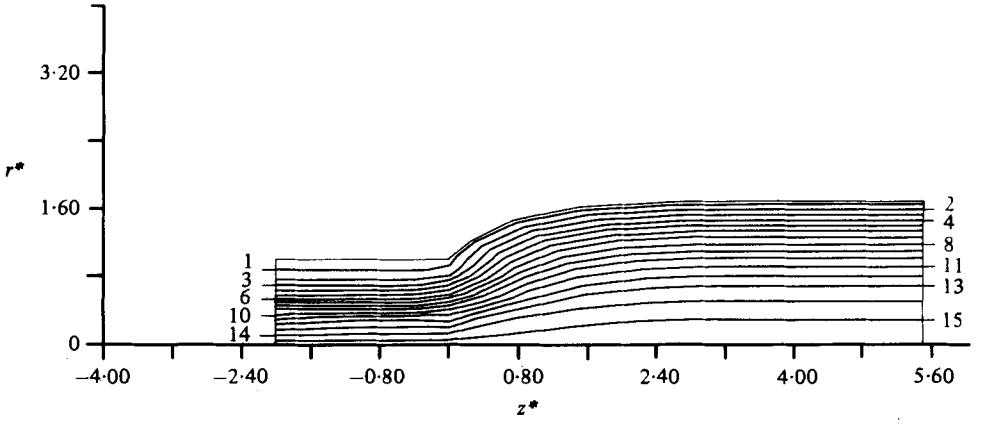

FIGURE 10. Streamlines for $\overline{w} = 30\,\mathrm{mm\,s^{-1}}$.

type of solid-rod analysis that leads to equation (31) and note that the solution takes the form

$$T = \sum_{n=1}^{\infty} J_0(\alpha_n r^*)\{A_n \exp z^*[Pe + (Pe^2 + \alpha_n^2)^{\frac{1}{2}}] + B_n \exp z^*[Pe - (Pe^2 + \alpha_n^2)^{\frac{1}{2}}]\} \quad (36)$$

with $Pe = \rho c \overline{w} R/k$ the Péclet number.

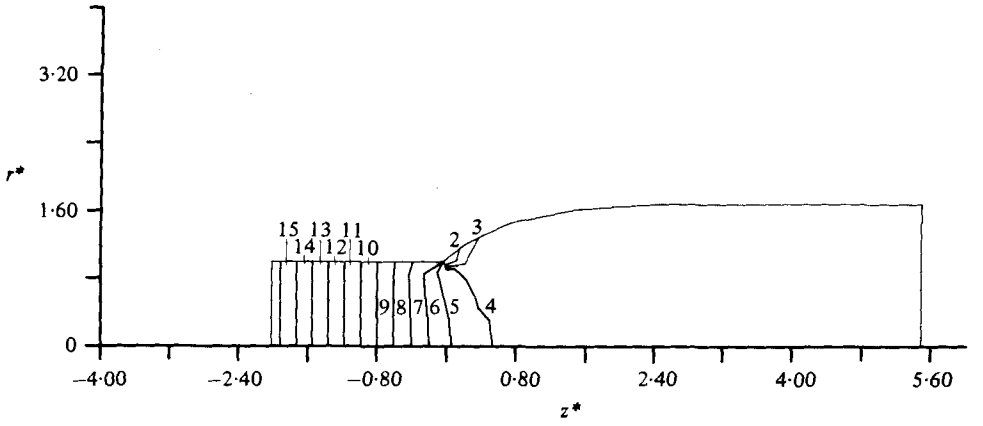

FIGURE 11. Dimensionless pressure (p^*) contours for $\bar{w} = 30\,\mathrm{mm\,s^{-1}}$. Note that at the exit plane, on the centre-line, there is a positive pressure. Values of p^* for the contours are: (1) −1·11; (2) −0·67; (3) −0·27; (4) 0·20; (5) 0·64; (6) 1·07; (7) 1·51; (8) 1·95; (9) 2·39; (10) 2·82; (11) 3·26; (12) 3·70; (13) 4·13; (14) 4·57; (15) 5·01.

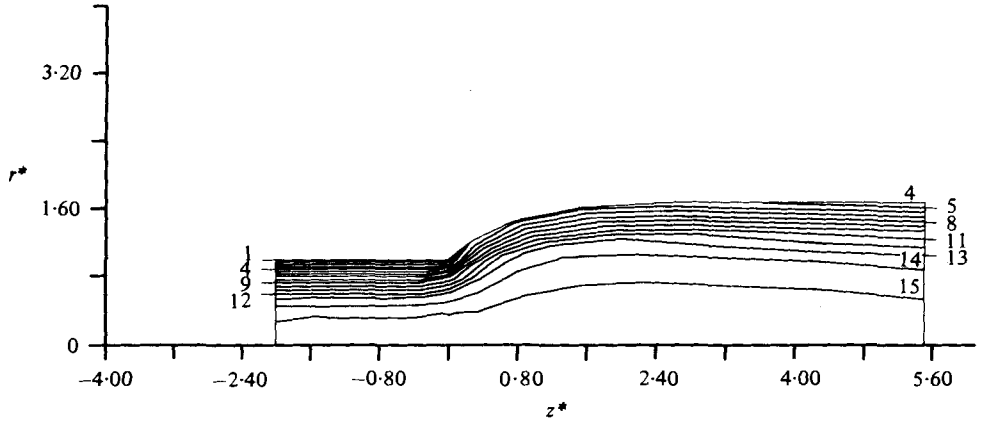

FIGURE 12. Dimensionless temperature (T^*) contours for $\bar{w} = 30\,\mathrm{mm\,s^{-1}}$. Contour (1) is for $T^* = 0{\cdot}020$, contour (15) is for $T^* = 0{\cdot}570$, and the contour interval is 0·0393.

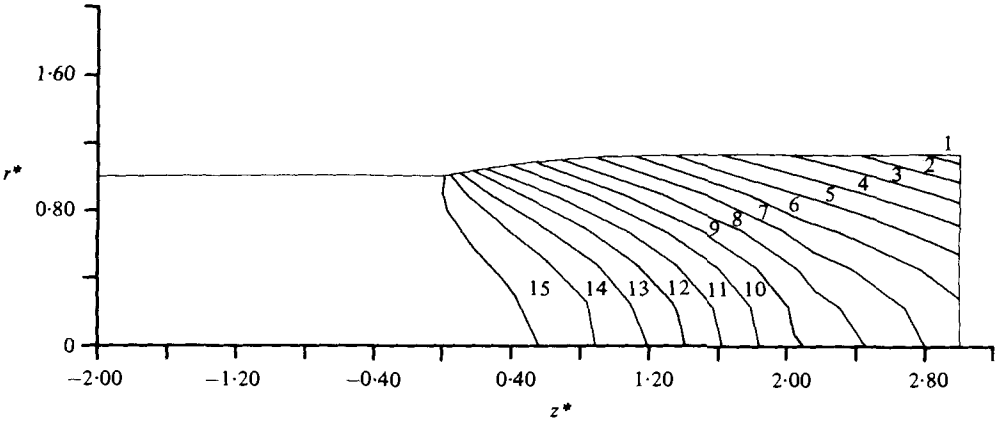

FIGURE 13. Dimensionless temperature (T^*) contours for $\bar{w} = 1\,\mathrm{mm\,s^{-1}}$. Contour (1) is for $T^* = -0{\cdot}526$, contour (15) is for $-0{\cdot}016$ and the contour interval is 0·0365.

The coefficients A_n and B_n should be evaluated from the conditions at $z^* = 0$ and $z^* = 3$. In the present case we find that the A_n are of order 10^{-18} (or less) times the B_n, (assuming the lowest Pe is 6·3) and hence the B_n are determined essentially entirely by the upstream conditions. The small 'kink' in a thin boundary layer which would be necessary to achieve the zero gradient condition is not visible with the mesh used. Hence, at the Péclet numbers considered, the present solution is accurate despite the arbitrary boundary condition assumption at the exit plane; the implied zero-gradient temperature boundary condition at $z^* = 3$ is ignored.

5. Discussion

The main results achieved here are the creation of a program that can handle coupled fluid mechanics and heat transfer problems in highly viscous liquids and the discovery of the thermal extrudate-swelling phenomenon. The computational scheme used here, where the temperature is solved for simultaneously with the mechanical variables, is not strictly necessary for the forced convection problems tackled so far; for example Gartling (1977) solves alternately for these variables. We have in mind the use of this type of scheme for future solutions of natural convection problems, however, and in this direction the present program will be useful. It would also be interesting to compare the speed of the two types of scheme. This has not been done so far.

Regarding the thermal swelling phenomenon, one can consider a dimensional analysis of the variables in the problem. We can write the expansion ϵ as

$$\epsilon = \epsilon(\bar{w}, R, \rho, \bar{\mu}, \alpha, \rho c, k, h, T_w - T_\infty). \tag{37}$$

Here we regard T_w as a reference for temperature level, and hence only $T_w - T_\infty$ enters the problem. From the above quantities we can form 5 dimensionless groups so that

$$\epsilon = \epsilon\left\{\frac{\rho\bar{w}R}{\mu}, \frac{\rho c\bar{w}R}{k}, \frac{hR}{k}, \frac{\alpha\mu\bar{w}^2}{k}, \frac{k(T_w - T_\infty)}{\bar{\mu}\bar{w}^2}\right\}. \tag{38}$$

In the solid rod problem, equation (31), we found that $\rho c\bar{w}R/k$ and hR/k occur separately, hence we have not combined them into a Stanton number, nor have we attempted to combine the other groups. Of these, the first (Reynolds) number is so small as to be irrelevant in the present investigation. The Nusselt number hR/k controls the rate of cooling of the extrudate. The last group is a temperature ratio comparing the temperature rise from the viscous effects to the temperature drop between the wall and the ambient temperature; it is also important in determining how fast the extrudate cools. The group containing α has been termed the Nahme–Griffith number (Pearson 1977). We give this group the symbol Na.

It has not been possible to explore the effects of these parameters fully but we may look for some limiting cases when the polymer is a good and a bad conductor of heat respectively. In the first case $k \to \infty$ and the fluid temperature will differ negligibly from the tube temperature everywhere; thus we return to the Newtonian swelling ratio. When k is small, the heat produced at a particle is not much diffused. In this case the convection boundary condition is not important ($Nu \to \infty$) and the surroundings temperature T_w is also not an important parameter in the problem. Hence we find

$$\epsilon = \epsilon(\alpha\bar{\mu}\bar{w}^2/k). \tag{39}$$

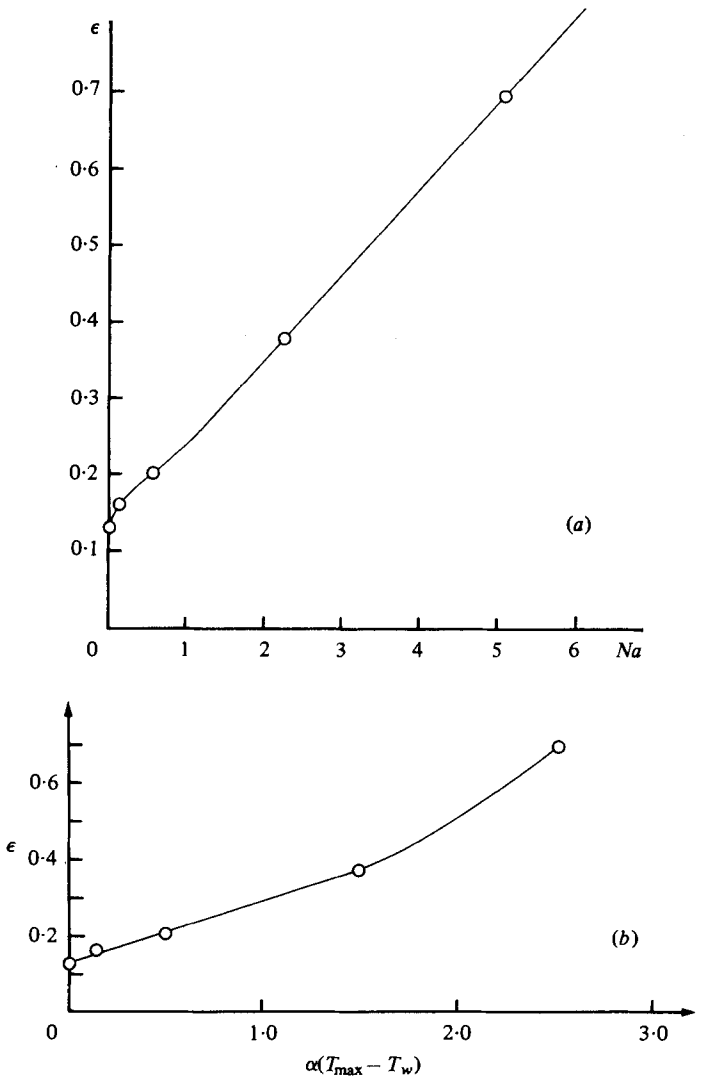

FIGURE 14. (*a*) Swelling ϵ as a function of the Nahme–Griffith number (Na). (*b*) Swelling ϵ as a function of α ($T_{\max} - T_w$), where $T_{\max}$ is the maximum temperature on the centre-line and T_w is the die wall temperature.

We believe the computations at the higher extension rates are close to this condition; heat conduction is unimportant except as a mechanism for setting up the initial temperature profile at the exit plane and enabling the final cooling of the rod to take place. One can look at figure 12 to see this and also to see that the surface heat loss is quite unimportant close to the exit in this case; hence the ambient temperature T_∞ is also a relatively unimportant parameter in this calculation. The Péclet number is large (~ 190) and thus we are in the large Pe régime where heat diffusion is not important (except for the setting up of the initial profile). We plot the results in the form (39) in figure 14(*a*). At the highest rates we have, approximately

$$\epsilon = 0{\cdot}129 + 0{\cdot}112\,Na \quad (Na \gg 1). \tag{40}$$

Diffusion is expected to reduce ϵ by reducing temperature differences in the extrudate; hence (40) appears to be a useful bound to the problem.

We note further that since the main function of the dissipation is to produce the initial temperature differential in the extrudate, we expect that the results obtained for swelling due to *any* method of producing a similar temperature distribution near the exit will be both qualitatively and quantitatively similar to the present results. Thus we can expect that shooting hot fluid into a cold, fairly short die will produce similar effects to those computed. To help with applications such as these, we may note from equation (29) that the maximum temperature on the axis ($T_{\max}$) when the viscosity is constant at $\bar{\mu}$, is given by

$$T_{\max} = T_w + \bar{\mu}\bar{w}^2/k. \tag{41}$$

Thus $T_{\max} - T_w$ is closely related to the parameter $\bar{\mu}\bar{w}^2/k$. Hence, as a rough approximation, we can write equation (41) in the more useful form

$$\epsilon = a + b\alpha(T_{\max} - T_w).$$

Figure 14 (*b*) shows this curve, and suggests that for moderate heating

$$\epsilon = 0{\cdot}129 + 0{\cdot}165\alpha(T_{\max} - T_w) \quad \text{if} \quad \alpha(T_{\max} - T_w) < 1{\cdot}6. \tag{42}$$

Since the Nahme–Griffith numbers reached in practical extrusion will often be of the order of these considered here, we recommend that this factor be taken into account when attempting to reconcile experiments with theories of extrusion. We are not aware of any experiments that could be compared to our results, but we feel that these would be of interest.

Finally, the problem of explaining these results has been undertaken in a new study (Tanner 1980). The theory of extrudate swell put forward there is based on the idea that the outer portion of the jet is being stretched and is in a state of tension. To preserve axial force equilibrium, it follows that the core of the extrudate must be in compression. When the viscosity of the outer layers is larger than that of the inner layers, as it is here, a small rate of outer layer extension is sufficient to balance core compression. Consideration of the mass balance over the jet then yields the result that the extrudate must expand. This theory agrees well with equation (42).

The authors are grateful to the Australian Research Grants Commission and to the University of Sydney for supporting this project.

REFERENCES

Acierno, D., Dalton, J. N., Rodriguez, J. M. & White, J. L. 1971 Rheological and heat transfer aspects of melt spinning of mono-filament fibres of polyethylene and polystyrene *J. Appl. Polymer Sci.* **15**, 2395.

Gartling, D. K. 1977 Convective heat transfer analysis by the finite element method. *Computer Methods in Appl. Mech. & Engng* **12**, 365.

Goren, S. L. & Wronski, S. 1966 The shape of low-speed capillary jets of Newtonian liquids. *J. Fluid Mech.* **25**, 185.

Kearsley, E. A. 1962 The viscous heating correction for viscometer flows. *Trans. Soc. Rheol.* **6**, 253.

Laskaris, T. E. 1975 Finite element analysis of compressible and incompressible viscous flow and heat transfer problems. *Phys. Fluids* **18**, 1639.

NICKELL, R. E., TANNER, R. I. & CASWELL, B. 1974 The solution of viscous incompressible jet and free-surface flows using finite-element methods. *J. Fluid Mech.* **65**, 189.

PHUOC, H. B. 1978 Solutions to some flow problems via a finite element method. M.Eng.Sc. thesis, University of Sydney.

PEARSON, J. R. A. 1977 Variable viscosity flows in channels with high heat generation. *J. Fluid Mech.* **83**, 191.

TANNER, R. I. 1970 A theory of die swell. *J. Polymer Sci.* A **8**, 2067.

TANNER, R. I. 1980 A new inelastic theory of extrudate swell. *J. Non-Newtonian Fluid Mech.* **6**, 289.

TANNER, R. I., NICKELL, R. E. & BILGER, R. W. 1975 Finite element methods for the solution of some incompressible non-Newtonian fluid mechanics problems with free surfaces. *Computer Methods in Appl. Mech. & Engng* **6**, 155.

TAY, A. O. & DE VAHL DAVIES, G. 1971 Application of the finite element method to convection heat transfer between parallel planes. *Int. J. Heat Mass Transfer* **14**, 1057.